

# OPTIMAL CURE CYCLES FOR MANUFACTURING OF THICK COMPOSITE PARTS USING MULTI-OBJECTIVE GENETIC ALGORITHMS

G. Struzziero<sup>1</sup>, J. Teuwen<sup>1</sup>

<sup>1</sup>Structural Integrity and Composites Group, Department of Aerospace Structures & Materials, Delft University of Technology, Kluyverweg 1, 2629 HS Delft, Netherlands  
Email:G.Struzziero@tudelft.nl

**Keywords:** Cure, Optimization, thick components, FE

## Abstract

The paper addresses the multi-objective optimization of the cure process of a Vacuum Assisted Resin Transfer Molding for components ranging from 40 to 100 mm thickness and aims to investigate the effect of thickness on the identification and quantification of a set of optimal cure profiles that minimize temperature overshoot and process time. Optimal cure solutions are sought among three dwells temperature profiles and are compared to the manufacturer's recommended cure cycle (MRCC). The methodology successfully approximates the efficient fronts for the three different cases under study (40, 70 and 100mm) and points out the efficiency opportunity available compared to MRCC. In the case of 70 and 100 mm thick component temperature overshoot reductions of about 75% are achievable and 67% reduction in process time. The results also suggest a change in the objectives' landscape for the higher thicknesses in the vertical region of the Pareto.

## 1. Introduction

As the complexity of geometry, production volumes and component size increase the composite manufacturing industry is driven towards more and more stringent requirements in terms of reliability, quality and efficiency. The cure stage of a thermoset composite manufacturing process involves several challenges that need to be addressed at design stage. In specific, the design of the cure cycle plays a vital role. Poorly designed cure cycles can lead to unnecessary long process time with direct consequences on process cost and to unwanted exothermic phenomena which lead to thermal gradients through thickness which result in residual stresses generation that are detrimental for the part quality and mechanical performances [1, 2]. This phenomenon becomes extreme in the case of thick and ultra-thick components where the combination of high thickness and low composite thermal conductivity through thickness generate violent temperature overshoot. The optimization of the cure cycle for the manufacturing of thick aerospace components [3, 4] and ultra-thick aerospace components [5, 6] has been addressed in literature to minimize process time. In the aerospace field, parts with thicknesses greater than 50 mm can be considered ultra-thick whilst thickness well below 10 mm are considered thin parts [7]. The optimization of the cure cycle to minimize residual stresses and part distortion has been addressed [8, 9]. Understanding the close relationship between process time and quality and their inverse dependence, researchers have tried to combine the two objectives in a more comprehensive way via weighted fitness function [10, 11]. However the selection of weights implies a prioritization between the different objectives and therefore the problem is equivalent to a single objective optimization with application of constraints achieving a limited exploration of the objectives and design space. A fully exploration and exploitation of both design and objectives space has been achieved via a pure multi-objective optimization methodology which unveiled the existence of Pareto front, i.e. trade-off, between process time and maximum temperature overshoot [7]. The thickness

influence on temperature overshoot and process time on Pareto front was also investigated but limited to thickness lower than 24mm and pointed out that higher thicknesses shifts the Pareto toward longer process time and higher temperature overshoots [12]. In the present paper the multi-objective optimization of the cure stage of ultra-thick components suitable for wind industry application is performed utilizing a methodology that combines a Genetic Algorithm (GA) with a Finite Element (FE) model of the cure process [7]. The paper investigates the cure profile selection problem for a Vacuum Assisted Resin Transfer Molding process to minimize both process time and maximum temperature overshoots and researches the effect of thickness on this selection. The paper pushes the limits of thickness range investigation across thick up to ultra-thick components in the range of 40-100 mm which corresponds to typical dimensions found in pure laminate wind turbine blades component. The chemical characterization of a widely used epoxy resin for wind energy application is also performed and the material models developed implemented in an FE cure simulation.

## 2. Material properties

The materials used in the study were E-glass fibers and Airstone 780E/785H epoxy resin [13]. The cure kinetics of the resin system has been characterized since there is no available data for the system in literature. The equipment utilized is a Perkin Elmer<sup>®</sup> Differential Scanning Calorimetry (DSC). One dynamic run at 1 °C/min and four isothermal tests at 50, 70, 90 and 110 °C have been performed. The experimental data have been fitted with a model that includes a diffusion limitation term as proposed by Khoun et al [14] and it is as follows:

$$\frac{d\alpha}{dt} = \frac{Ae^{\left(\frac{-E}{RT}\right)}}{1 + e^{C(\alpha - \alpha_c - \alpha_T T)}} (1 - \alpha)^n \alpha^m \quad (1)$$

here  $\alpha$  is the degree of cure,  $n$ ,  $m$  reaction orders,  $A$  pre-exponential Arrhenius coefficient,  $E$  the activation energy,  $R$  the universal gas constant,  $\alpha_c$  and  $\alpha_T$  are coefficients controlling the transition of the kinetics from chemical to diffusion control. Fig. 1 reports the experimental data and the fitting with the model proposed whilst the fitting parameters are reported in Table 1.

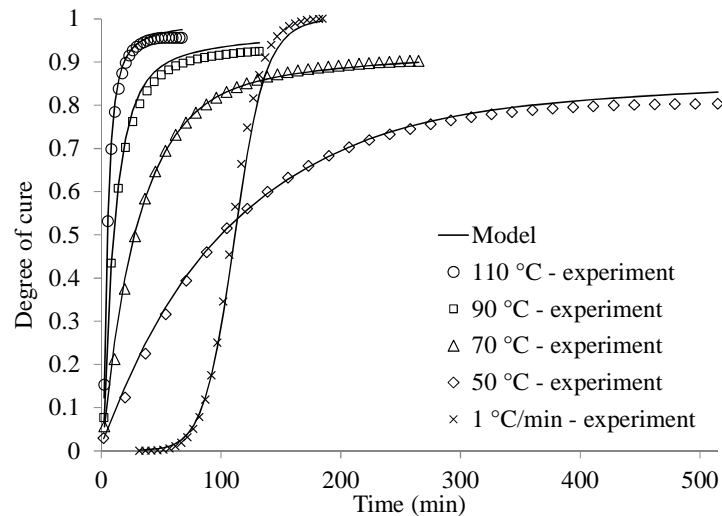


**Figure 1.** Cure kinetics model fitting for Airstone<sup>™</sup> 780E/785H system

In order to verify the assumption that the cure kinetics of the system under study could be described as a function of temperature and degree of cure and that thermal history does not play an important role a superposition test [15] has been carried out. The test consists in comparing reaction rates measured at the same points of the conversion-temperature phase space, by isothermal and dynamic tests. The superposition of data from dynamic and isothermal tests is reported in Fig. 2. The reaction rate obtained from the dynamic test is very close to the ones obtained from isothermal test. Therefore thermal history does not play a role for the resin system investigated and the system can be modelled as a unique function depending on conversion and temperature.

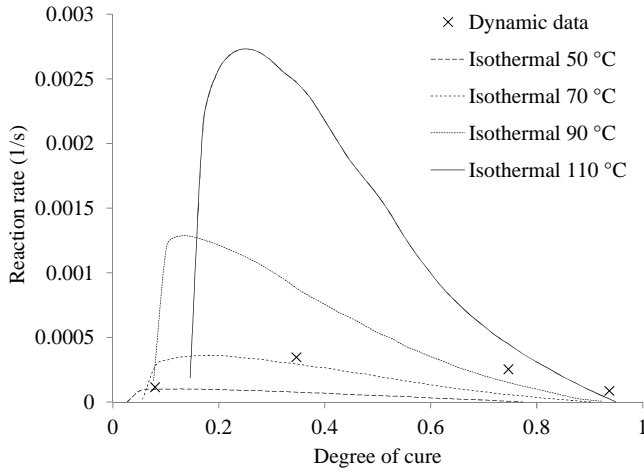


**Table 1.** Cure kinetics fitting parameters

Airstone <sup>TM</sup> 780E/785H	
$A$ ( $s^{-1}$ )	1474423
$E$ ( $J mol^{-1}$ )	61763
$n$	1.657
$m$	0.069
$C$	30.7
$\alpha_c$	0.64
$\alpha_T$ ( $K^{-1}$ )	0.029
$H_{tot}$ ( $J g^{-1}$ )	435

**Figure 2.** Superposition test results

The glass transition temperature evolution of the system has also been measured using partially cured samples. The samples were heated in the DSC equipment at 1 °C/min up to increasing final temperatures and quickly cooled down after reaching the desired temperature in order to stop the cure. A subsequent run at 10 °C/min was run to identify the glass transition temperature using the step in heat flow observed. A number of three repeated test per final temperature were undertaken. The data reported can be modelled using the Di Benedetto equation [16] which is as follows:

$$T_g = T_{g0} \frac{(T_{g\infty} - T_{g0}) \lambda \alpha}{1 - (1 - \lambda) \alpha} \quad (2)$$

where  $T_{g0}$  is the glass transition temperature of the uncured material,  $T_{g\infty}$  of the fully cured and  $\lambda$  is a fitting parameter governing the convexity of the dependence of degree of cure and glass transition temperature. The experimental data and the fitting with the model is illustrated in Fig. 3 whilst the fitting parameter for the Di Benedetto equation are reported in Table 2.

The specific heat of the composite is calculated using the rule of mixtures:

$$c_p = w_f c_{pf} + (1 - w_f) c_{pr} \quad (3)$$

where  $w_f$  is the weight fraction of the fiber (0.70),  $c_{pf}$  the specific heat of the fibers and  $c_{pr}$  the specific heat of the resin. The specific heat of glass fibers follows a linear dependence on temperature whilst the resin depends on both temperature and degree of cure [7, 17]:

$$c_{pf} = A_{fcp} T + B_{fcp} \quad (4)$$

$$c_{pr} = A_{rcp} T + B_{rcp} + \frac{\Delta_{rcp}}{1 + e^{C_{rcp}(T - T_g - \sigma)}} \quad (5)$$

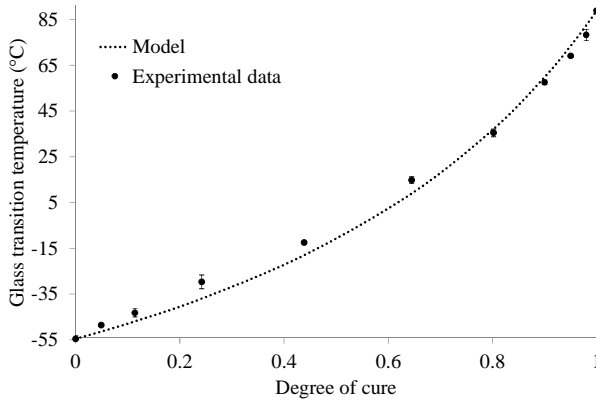


**Table 2.** Di Benedetto model fitting parameters

Airstone™ 780E/785H	
$T_{g0}$ (°C)	-55
$T_{g\infty}$ (°C)	89
$\lambda$	0.437

**Figure 3.** Di Benedetto model for Airstone™ 780E/785H

Here  $A_{fcp}$  is equal to 1.4 J/Kg°C<sup>2</sup>,  $B_{fcp}$  is equal to 841 J/Kg°C and represent the slope and the intercept of the linear dependence of fiber specific heat capacity on temperature,  $A_{rcp}$ ,  $B_{rcp}$  are constants expressing the linear dependence of the specific heat capacity of the uncured epoxy on temperature and  $\Delta_{rcp}$ ,  $C_{rcp}$  and  $\sigma$  are the strength, width and temperature shift of the step reduction in specific heat capacity at vitrification. The thermal conductivity of the composites can be evaluated as follows for longitudinal ( $K_{11}$ ) and transverse ( $K_{22}$ ) direction [18]:

$$K_{11} = v_f K_{tf} + (1 - v_f) K_r \quad (6)$$

$$K_{22} = K_{33} = v_f K_r \left( \frac{K_{tf}}{K_r} - 1 \right) + K_r \left( \frac{1}{2} - \frac{K_{tf}}{2K_r} \right) + K_r \left( \frac{K_{tf}}{K_r} - 1 \right) \sqrt{v_f^2 - v_f + \frac{\left( \frac{K_{tf}}{K_r} + 1 \right)^2}{\left( \frac{2K_{tf}}{K_r} - 2 \right)^2}} \quad (7)$$

where  $K_{lf}$ ,  $K_{tf}$  represents the longitudinal and transverse thermal conductivity of the fibers which for the E-glass fibers are the same and equal to 1.03 W/m°C [19] and  $K_r$  which is the thermal conductivity of the resin and can be represented as follows [20]:

$$K_r = a_{Kr} T \alpha^2 + b_{Kr} T \alpha + c_{Kr} T + d_{Kr} \alpha^2 + e_{Kr} \alpha + f_{Kr} \quad (8)$$

where  $a_{Kr}$ ,  $b_{Kr}$ ,  $c_{Kr}$ ,  $d_{Kr}$ ,  $e_{Kr}$  and  $f_{Kr}$  are coefficients of the polynomial function. The glass fibers values and resin values adopted for the evaluation of specific heat and thermal conductivity of the composite are taken from literature [7, 17, 20]

### 3. Cure simulation

The coupled thermo-chemical solution of the heat transfer problem has been modelled and solved using the FE solver Marc.Mentat<sup>®</sup> [21]. The three-dimensional 8-nodes brick composite elements for heat transfer analysis were used [22]. Time dependent fixed temperature boundary conditions have been implemented using FORCDT user subroutine at the nodes in contact with the mold whilst air convection boundary condition has been applied on the vacuum bag side via UFILM user subroutine [23]. The convection heat transfer coefficient has been assumed equal to 13.6 W/m<sup>2</sup>K [24]. Initial temperature condition has been set equal to 25 °C. The model has been implemented using a 3D analysis; however the heat transfer problem is one dimensional. This is achieved by using one layer of

elements in the in-plane direction which together with the zero heat flux boundary condition results in an infinite length in this direction. The sub material models for cure kinetics, specific heat and thermal conductivity have been implemented via user subroutine UCURE, USPCHT and ANKOND [23]. Fig. 4 reports a schematic illustrating the boundary conditions applied.

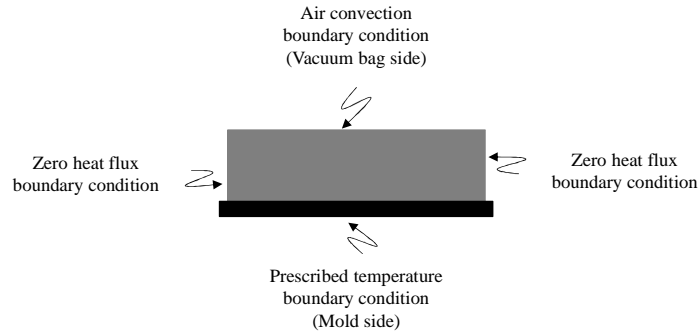
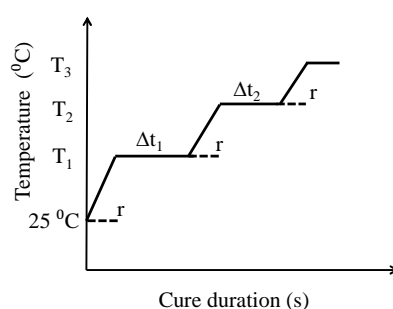


**Figure 4.** Model boundary conditions

#### 4. Multi-objective optimization of the cure

The aim of the multi-objective optimization is to minimize both process time and maximum temperature overshoot by finding a set optimal cure profiles. The optimization methodology used a GA able to deal with multi-objective problems which via an interface written in C++ communicates with the FE solver updating the input file before each simulation run. A detailed description of the interface can be found in [7]. A total of three test cases have been considered. The geometry chosen is a flat panel with thicknesses spanning from thick up to ultra-thick component in specific 40, 70 and 100 mm have been taken into account. The model is made of 16 elements through thickness. The layup is unidirectional and the volume fiber fraction 54%. The solution due to symmetry is one dimensional in thickness direction. A three-dwell cure profile has been identified as suitable due to the high thicknesses at play [25]. The cure profile has been parametrized into six parameters; temperature of the first, second and third dwell ( $T_1$ ,  $T_2$ ,  $T_3$ ), the duration of first and second dwell ( $\Delta t_1$ ,  $\Delta t_2$ ) and the ramp rate ( $r$ ). The general shape of the cure profile is illustrated in Fig. 5 a) whilst the ranges of the cure profile parameters are reported in Fig. 5 b). It needs to be pointed out that the third dwell duration is not a design parameter. This comes directly from the definition of cure process duration as the time at which the minimum degree of cure within the model reaches the target of 92%. This is the minimum degree of cure reached by the 100 mm thick flat panel when the MRCC is applied. The MRCC involves a ramp up to 70 °C at 0.33 °C/min ramp rate followed by 4 h at 70 °C [13]. The optimization parameters for the optimizer has been fine-tuned for the problem under study and reported in Table 3. A maximum number of generations have been set although the convergence might occur at earlier generations.



a)

Parameters	Ranges
$T_1$ (°C)	30-70
$T_2$ (°C)	70-110
$T_3$ (°C)	110-130
$\Delta t_1$ (min)	5-180
$\Delta t_2$ (min)	5-180
$r$ (°C/min)	0.1-4

b)

**Figure 5.** Parameterized cure profile a) General shape b) Design parameters range

**Table 3.** GA parameters used for cure optimization.

GA input	
Max Number of generations	10
Individuals per population	60
Individuals per reproduction	48
Elite individuals	4
Size of Pareto set	40
Mutation probability	0.005
Cross-over probability	0.5

## 5. Results and discussion

Fig. 6 depicts the results from the multi-objective optimization. Fig. 6 a) reports the optimization results regarding the 40 mm thick, b) the 70 mm thick and c) the 100 mm thick flat panel and all include the results when applying the MRCC to this thickness. In Fig. 6 d) a comparison of the three different thicknesses results is illustrated. The results show that the optimization methodology successfully identified and quantified the existing trade-offs between the objectives. The trade-offs are in the form of an L-shape which highlights the competitive nature of the objectives. However, at low process time the L-shape Pareto of ultra-thick laminate (70 and 100 mm) shows less dependence between the two objectives and overlaps from 5000 s process time and lower, suggesting a change in the problem landscape for ultra-thick components in the vertical region of the L-shape Pareto. By adopting cure profiles found by the optimization methodology significant benefits can be achieved both in process time and temperature overshoot reduction. Regarding the 40 mm flat panel reduction of about 50% in temperature overshoot and 80% in process time are achieved compared to MRCC. In the 70 and 100mm flat panel about 75% reduction in temperature overshoot can be achieved and about 68% reduction in process time making the implementation of the optimization methodology necessary in the case of ultra-thick components. From the comparison of the final efficient front found by the optimization it can be noticed that higher thicknesses shifts the efficient front towards longer process time and higher temperature overshoot temperature which is in agreement with [12]. However, the overlapping of the two ultra-thick Pareto fronts at low process time and non-linear differences in the distance between the 40 and 100 mm Pareto with respect to the 70 mm Pareto were found in this work and are worth further research. These phenomena seem to suggest the existence of a threshold in thickness that dictates a change in the objectives relationship.

### 3. Conclusions

The optimization procedure presented in the paper is capable to identify a set of optimal cure profiles that can bring significant benefits compared to the result obtained applying MRCC in both objectives. The methodology proved to be suitable to identify optimal trade-off between the objectives in a broad range of thicknesses variation. The multi-objective setting allows the two objectives to be treated independently without implying their importance a priori unlike weighted fitness functions where the benefits of each objectives are assumed by the designer running the risk of hiding optimal solutions. Furthermore the paper highlights that MRCC are over conservative in terms of process time and also fail in keeping the overshoot temperature low in the ultra-thick cases during the process with consequences on part quality. Furthermore the paper suggests a change in objectives landscape for ultra-thick components in the vertical region of the Pareto front. Further work will involve the validation of the heat transfer model and the solution of the thermo-mechanical problem which will allow direct minimization of residual stresses.

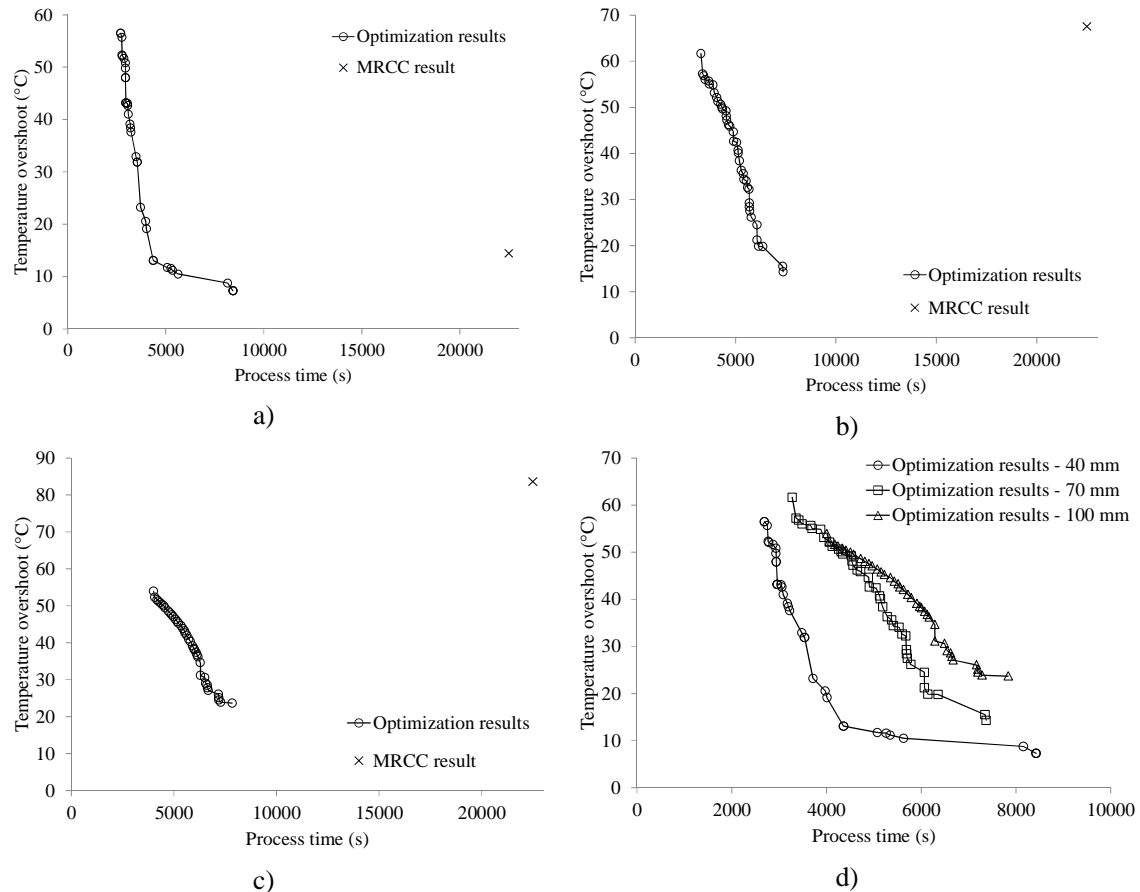


**Figure 6.** Flat panel optimization results a) 40 mm b) 70 mm c) 100 mm d) Thickness comparison

## Acknowledgments

This work was supported by the ADEM Innovation Lab.

## References

- [1] V. Antonucci, M. Giordano, K.T. Hsiao, S.G. Advani. A methodology to reduce thermal gradients due to the exothermic reactions in composites processing. *International Journal of Heat and Mass Transfer*, 45:1675-1684, 2002.
- [2] L. Esposito, L. Sorrentino, F. Penta, C. Bellini. Effect of curing overheating on interlaminar shear strength and its modelling in thick FRP laminates. *International Journal of Advanced Manufacturing Technology*, 87:2213-2220, 2016.
- [3] V. Pillai, A.N. Beris, P. Dhurjati. Heuristics guided optimization of a batch autoclave curing process. *Computers and Chemical Engineering*, 20:275-294, 1996.
- [4] N. Rai, R. Pitchumani. Optimal cure cycles for the fabrication of thermosetting-matrix composites. *Polymer Composites*, 18:566-581, 1997.
- [5] Z.L. Yang, S. Lee. Optimized curing of thick section composite laminates. *Materials and Manufacturing Processes*, 16:541-560, 2001.
- [6] P. Carlone, G.S. Palazzo. A simulation based metaheuristic optimization of the thermal cure cycle of carbon epoxy composite laminates. *Proceedings of The 14th International ESAFORM Conference on Material Forming, Belfast, United Kingdom*, April 27-29 2011.

- [7] G. Struzziero, A.A. Skordos. Multi-objective optimisation of the cure of thick components. *Composites Part A*, 93:126-136, 2017.
- [8] Q. Zhu, P.H. Geubelle. Dimensional accuracy of thermoset composites: Shape optimization. *Journal of Composite Materials*, 36:647-672, 2002.
- [9] A.K. Gopal, S. Adali, V.E. Verijenko. Optimal temperature profiles for minimum residual stress in the cure process of polymer composites. *Composite Structures*, 48:99-106, 2000.
- [10] E. Ruiz, F. Trochu. Multi-criteria thermal optimization in liquid composite molding to reduce processing stresses and cycle time. *Composites Part A*, 37:913-924, 2006.
- [11] N.G. Pantelelis. Optimised cure cycles for resin transfer moulding. *Composites Science and Technology*, 63:249-264, 2003.
- [12] G. Struzziero, A.A. Skordos. Multi-objective optimisation of composites cure using genetic algorithms. *ECCM15 – 15<sup>th</sup> European Conference on Composite Materials, Venice, Italy, June 24-28 2012*.
- [13] Airstone<sup>TM</sup> Infusion System Product Data. [www.dowepoxysystems.com](http://www.dowepoxysystems.com).
- [14] L. Khoun, T. Centea, P. Hubert. Characterization methodology of thermoset resins for the processing of composite materials - Case study: CYCOM 890RTM epoxy resin. *Journal of Composite Materials*, 44:1397-1415, 2010.
- [15] A.A. Skordos, I.K. Partridge. Cure kinetics of epoxy resins using a non parametric numerical procedure. *Polymer Engineering and Science*, 41:793-805, 2001.
- [16] J.P. Pascault, R.J.J. Williams. Glass transition temperature versus conversion relationships for thermosetting polymers. *Journal of Polymer Science*, 28:85-95, 1990.
- [17] A.A. Skordos. Modelling and monitoring of resin transfer moulding. *PhD thesis*. 2000.
- [18] J. Farmer, E. Covert. Thermal conductivity of a thermosetting advanced composite during its cure. *Journal of Thermophysics and Heat Transfer*, 10:467-475, 1996.
- [19] Q.C. Ning, T.W. Chou. A closed-form solution of the transverse effective thermal conductivity of woven fabric composites. *Journal of Composite Materials*, 29:2280-2294, 1995.
- [20] A.A. Skordos, I.K. Partridge. Inverse heat transfer for optimization and on-line thermal properties estimation in composite curing. *Inverse Problems in Science and Engineering*, 12:157-172, 2004.
- [21] Marc.Mentat<sup>®</sup> volume A: Theory and user information. [www.mssoftware.com](http://www.mssoftware.com), 2015.
- [22] Marc.Mentat<sup>®</sup> volume B: Element library. [www.mssoftware.com](http://www.mssoftware.com), 2015.
- [23] Marc.Mentat<sup>®</sup> volume D: User subroutines and special routines. [www.mssoftware.com](http://www.mssoftware.com), 2015.
- [24] T.S. Mesogitis, A.A. Skordos, A.C. Long. Stochastic heat transfer simulation of the cure of advanced composites. *Journal of Composite Materials*, 50:2971-2986, 2016.
- [25] K. Zimmermann, B. Van Den Broucke. Assessment of process-induced deformation and stresses in ultra thick laminates using isoparametric 3D elements. *Journal of Reinforced Plastics and Composites*, 31:163-178, 2011.